P10.1 AN ANALYTICAL MODEL OF ONE- AND TWO-CELLED VORTICES: PRELIMINARY TESTING

Vincent T. Wood[1], Luther W. White[2], Curtis R. Alexander[3], and Robin L. Tanamachi[3]
[1]NOAA/OAR/National Severe Storms Laboratory, [2]Department of Mathematics,
[3]School of Meteorology, University of Oklahoma
Norman, Oklahoma

1. INTRODUCTION

Tangential winds in atmospheric vortices (dust devils, tornadoes, mesocyclones, and other types of atmospheric vortices) are often approximated by continuous functions that are zero at the vortex center, increase to a maximum at core radius, and then decrease asymptotically to zero infinitely far from the center. Some observed tangential profiles resemble those of (a) the inviscid Rankine (1901) combined vortex (consisted of an inner core of solid-body rotation and an outer region of potential flow), (b) the viscous, one-celled Burgers (1948)-Rott (1958) vortex (characterized by fluid spiraling in toward the z -axis as it rises), and (c) the viscous, two-celled Sullivan (1959) vortex (consisted of sinking air along this axis which recirculates in an inner cell and rising motion in surrounding outer cell).

Proximity radar observations of tornadoes by mobile Doppler radars show that the wind profiles are different from one vortex to another during different stages. The radial profiles of Doppler velocities, in some cases, closely match those of inner cores of solid-body rotation. Outside the cores, the Doppler velocity profiles of $v_t \propto r^{-0.6\pm0.1}$ have been observed (e.g., Wurman and Gill 2000, Wurman 2002; Wurman and Alexander 2005). Some azimuthally-averaged tangential velocity profiles derived from W-band Doppler radar measurements (Tanamachi et al. 2006) resemble the Burgers (1948)-Rott (1958) vortex. The W-band Doppler radar-derived velocity profile of a Texas dust devil (Bluestein et al. 2004) is a good example of the Sullivan (1959) vortex.

The purpose of this study is to develop a new analytical model which permits one to dictate radial variations of tangential velocity component that characterize one- and two-celled vortices. The model does not include complex structures such as asymmetrics, multiple vortices, and vortex breakdowns. Vertical vorticity and the radius at which maximum vorticity occurs can analytically be derived from a mathematical function that describes the varying tangential velocity profiles. Least squares fits of model parameters to Doppler-analyzed and -derived tangential wind profiles provide evaluation of the parameters' distributions and critical examination of the profile's realism. Mobile Doppler radar measurements of the 30 May 1998 Spencer, South Dakota and the 15 May 1999 Stockton, Kansas tornadoes are used to test against the fitted parameters of the analytical model. Due to limited space in this paper, radial wind profiles are not presented.

Corresponding author address: Vincent T. Wood, National Severe Storms Laboratory, 120 David L. Boren, Blvd., Norman, OK 73072. E-mail: Vincent.Wood@noaa.gov

2. PARAMETRIC PROFILES

a. Tangential velocity

In an attempt to determine the degrees of varying tangential wind profiles in atmospheric vortices, a new analytical model is presented. The model employs four parameters: maximum tangential wind (V_x), core radius (R_x) at which maximum tangential wind occurs, k which dictates the concavity of the tangential velocity profile near the vortex center, and n which controls the decay rate of the profile (i.e., rate at which tangential velocity decays with increasing radial distance, r, outside the core). The radial variation of tangential velocity (v_t) is given by

$$v_t(r, V_x, R_x, k, n) = V_x \Phi(r, R_x, k, n), \quad (1)$$

where the continuous, dimensionless function Φ is expressed as

$$\Phi(r, R_x, k, n) = \frac{n R_x^{2(n-k)} r^{2k}}{(n-k) R_x^{2n} + k r^{2n}}, \quad (2)$$

where $0 < k < n$. A complete derivation of Eq. (2) is not presented due to limited space.

A family of the curves for the n and k values is presented in Fig. 1. When $k < 1/2$ and n is fixed, the tangential velocity profile near the vortex center has negative curvature as the curvature turns to right with increasing r (Fig. 1a). For $k = 1/2$, the profile has zero curvature at any point of a straight line near the center. When $k > 1/2$, the profile has positive (negative) curvature near the center (the core radius) as the curvature turns to left (right) with increasing r. Beyond a normalized core radius ($r/R_x > 1$), the k values have small effects on the tangential velocity profiles. By keeping k constant (Fig. 1b), increasing the n values increases the decay rate, while at the same time, the values slightly affect the profiles inside R_x.

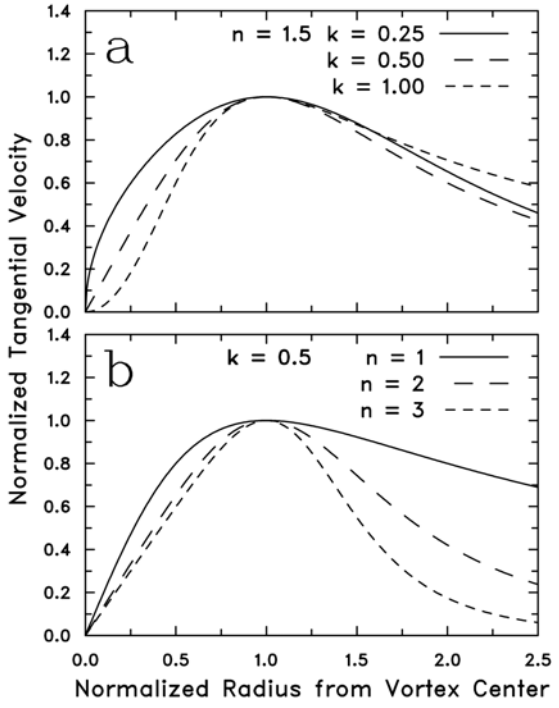

Fig. 1. Normalized tangential velocity (v_t/V_x) profiles as a function of the n and k values and normalized radius (r/R_x).

b. Vertical vorticity

Vertical vorticity (ζ) in axisymmetric flow is given by

$$\zeta = \frac{1}{r}\frac{\partial(v_t r)}{\partial r} = \frac{\partial v_t}{\partial r} + \frac{v_t}{r}. \qquad (3)$$

Substitution of Eqs. (1) and (2) into Eq. (3) yields

$$\zeta = V_x \frac{\Phi}{r}\left\{1 + 2k\left[1 - \Phi\frac{r^{2(n-k)}}{R_x^{2(n-k)}}\right]\right\}. \quad (4)$$

The radius ($R_{\zeta_{\max}}$) at which maximum ζ occurs is obtained by differentiating Eq. (4) with respect to r and setting $\partial\zeta/\partial r$ to zero. Thus, the resultant is given by

$$ar^{4n} + br^{2n} + c = 0, \quad n \neq 0, \qquad (5)$$

where the coefficients are:

$a = k^2[4(n-k)^2 - 1]$,

$b = 2k(n-k)[-4k(n-k) - 2n^2 - 1]R_x^{2n}$,

and,

$c = (4k^2 - 1)(n-k)^2 R_x^{4n}$.

$R_{\zeta_{\max}}$ can easily be obtained using the quadratic formula since Eq. (5) is quadratic in r^{2n} and is given by

$$R_{\zeta_{\max}} \equiv r = \left(\frac{-b \pm \sqrt{b^2 - 4ac}}{2a}\right)^{1/2n}, \quad a \neq 0,$$

and $n \neq 0$. (6)

In Eq. (6), there are two distinct real roots for $R_{\zeta_{\max}}$ and the discriminant of the quadratic equation is found to be positive since $b^2 > 4ac$. Since $R_{\zeta_{\max}} < R_x$, one can choose only one explicit solution of $R_{\zeta_{\max}}$. That is,

$$R_{\zeta_{\max}} = \left(\frac{-b - \sqrt{b^2 - 4ac}}{2a}\right)^{1/2n}, a \neq 0,$$

$n \neq 0$, $1/2 < k < n$, (7a)

and $R_{\zeta_{\max}} = 0$, $0 < k \leq 1/2$. (7b)

When $n - k = 1/2$, $a = 0$ in Eq. (5) so that the equation can be simplified by eliminating the first term on the left-hand side of Eq. (5) and is given by

$$R_{\zeta_{\max}} = \left(-\frac{c}{b}\right)^{1/2n}, \quad 1/2 < k < n,$$

and $R_{\zeta_{\max}} = 0$, $0 < k \leq 1/2$. (8)

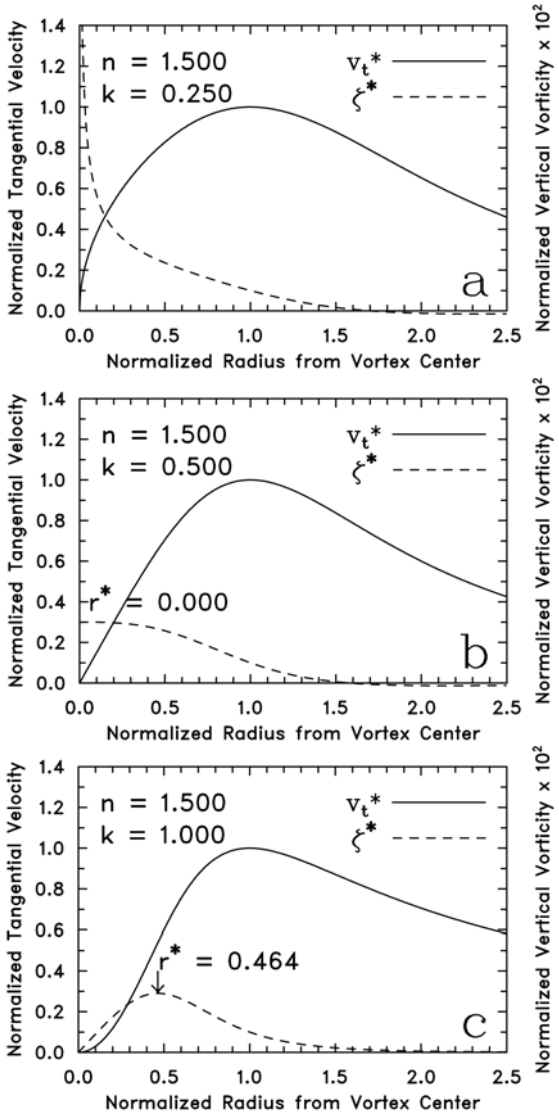

Fig. 2. Normalized tangential velocity ($v_t^* = v_t / V_x$, solid curve) and vertical vorticity ($\zeta^* = \zeta r / V_x$, dashed curve) as a function of the normalized radius (r / R_x) and the k values while n is fixed.

A family of normalized vertical vorticity (dashed) curves for the k values corresponding to the normalized tangential velocity profiles (Fig. 1) is illustrated in Fig. 2. When $k < 1/2$, ζ^* approaches infinity as $r^* = R_{\zeta_{\max}} / R_x \to 0$ (Fig. 2a). When $k = 1/2$, maximum ζ^* occurs at $r^* = 0$ with the profile being bell-shaped (Fig. 2b). This profile suggests that the one-celled vortex is barotropically stable (Davies-Jones 1986). When $k > 1/2$, an annulus of maximum ζ^* always occurs at $0 < r^* < 1$, while being displaced away from the vortex axis toward the strongest gradient of the profile inside the core radius (Fig. 2c). This annular pattern of ζ^* is characteristic of a two-celled structure (e.g., Rotunno 1977, 1984; Bluestein et al. 2004; Lee and Wurman 2005). This vorticity profile satisfies the necessary (but not sufficient) condition of barotropic instability (Davies-Jones 1986). Multiple vortices occur in concentrated vertical vorticity located in an annular region between the cells.

3. PROFILE FITTING

Least squares fits of four model parameters (V_x, R_x, n, and k) to Doppler wind profiles permit us to evaluate the parameters' distributions and critical examination of the profile's realism. We seek the solutions of the parameters that yield the minimum value of a cost function $J(\mathbf{m})$. We take $\mathbf{m} = [V_x, R_x n, k]^t$ to be a vector of four model parameters. The cost function for the minimization is

$$J(\mathbf{m}) = \Sigma \left[V(\mathbf{m}) - \tilde{V} \right]^2 , \qquad (9)$$

where $V(\mathbf{m})$ is an optimal tangential velocity component as a function of the model vector $\mathbf{m}$, and $\tilde{V}$ is the Doppler radial velocity data. Eq. (9) is the summed squares of the differences between the modeled and observed tangential wind profiles. We followed the least squares technique of Gerald and Wheatley (1984) to obtain the fitted model parameters. Initial maximum tangential velocity (V_x) and core radius (R_x) are readily determined by scanning through a Doppler wind profile. Initial guesses of n and k are 1.0 and 0.5, respectively.

4. CASE STUDIES

a. 30 May 1998 Spencer, South Dakota tornado

On the evening of 30 May 1998, a supercell moved across southeastern South Dakota and produced at least one strong and one violent tornado, the latter of which passed through the town of Spencer (Alexander and

Wurman 2005). The F4 tornado was intercepted by the Doppler On Wheels (DOW) mobile radar, from a range of 1 to 8 km, resulting in high-resolution volumetric data at low elevation angles over a period of 45-min.

Figure 3 presents a radial profile of Doppler tangential wind speed from the tornado center. The observed profile (as indicated by a black, dot-line curve) is the same as that in Fig. 6a of Wurman and Alexander (2005). The profile is compared to the analytical tangential velocity profile. The root-mean-square (RMS) error used to estimate the effectiveness of least-squares fitting between the observed and fitted profiles is 4.59 m s^{-1}. The observed profile is used to calculate vertical vorticity with the aid of Eq. (3) and Doppler tangential wind speed data. The observed vertical vorticity profile is compared to that of the vertical vorticity readily calculated from Eq. (4). When the inherent noisiness of the radar data is taken into account, these profiles show good agreement.

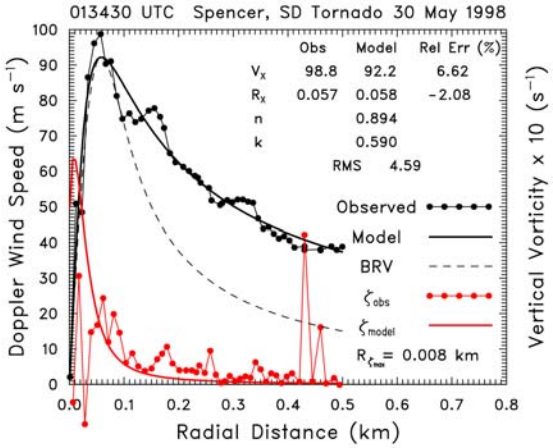

Fig. 3. Radial profiles of DOW-based Doppler wind speed (black dot-line curve) and analytical (black, solid curve) tangential velocity with corresponding observed (red, dot-line curve) and analytical (red, solid curve) vertical vorticity at 01:34:30 UTC. Dashed curve refers to the Burgers (1948)-Rott (1958) tangential velocity profile for comparison purpose. Relative errors (%) and RMS errors (m s^{-1}) between the observed and model parameters are indicated.

b. 15 May 1999 Stockton, Kansas tornado

High-resolution radar reflectivity and Doppler velocity data of the Stockton, Kansas tornado of 15 May 1999 were collected by a mobile, 3-mm-wavelength, 95-GHz (W-band) Doppler radar (Tanamachi et al. 2006). Data collection contained thirty-five scans of radar reflectivity and velocity data during the entire life cycle of the Stockton tornado. Throughout the collection period, the F1 tornado traveling towards the north-northwest was located 4-7 km west and west-northwest of the mobile Doppler radar.

Tanamachi et al. (2006) investigated the temporal evolution of the quasi-axisymmetric structure of the Stockton tornado at the level of the radar scan. They applied the Ground-Based Velocity Track Display (GBVTD, Lee et al. 1999) analysis technique to the Doppler radar data. From the technique, axisymmetric components of tangential and radial wind as well as the wavenumber-1, -2, and -3 angular harmonics of the tangential wind were generated.

Radial profiles of GBVTD-analyzed azimuthally-averaged and analytical tangential velocities are shown in Fig. 4. The profiles resemble the BRV's tangential velocity profile (dashed curve). Inside R_x, the slope of the velocity profile does not appear to follow solid-body rotation because the k value of 0.31 (0.73) indicates that the profile near the vortex center has negative (positive) curvature as the curvature turns to right (left) with increasing radial distance. (It is important to note that the GBVTD-analyzed velocities are regarded with reduced confidence at small radii because relatively few Doppler radar data points are used in the GBVTD analysis.) Least squares fits of four model parameters (V_x, R_x, n, and k) to GBVTD-analyzed tangential wind profiles show very good agreements with the observed profiles. The RMS errors in Fig. 4 are less than 1.0 m s^{-1}.

With the retrieved model parameters available, ζ and $R_{\zeta_{\max}}$ can analytically be estimated and are presented in Fig. 4. The calculated vertical vorticity is compared to the analytical vertical vorticity, suggestive of a one-celled vortex (Fig. 4a) and a two-celled vortex (Fig. 4b). This, however, is questionable because of a lack of data points inside R_x. No multiple vortices were visually observed in the Stockton tornado. Based on the W-band radar data, very short-lived multiple vortices, however, may have been present at ranges of 30-330 m from the

tornado center between 19:59:55 and 20:04:01 CDT. The fitted profile of ζ shows good agreement with the GBVTD-analyzed profile.

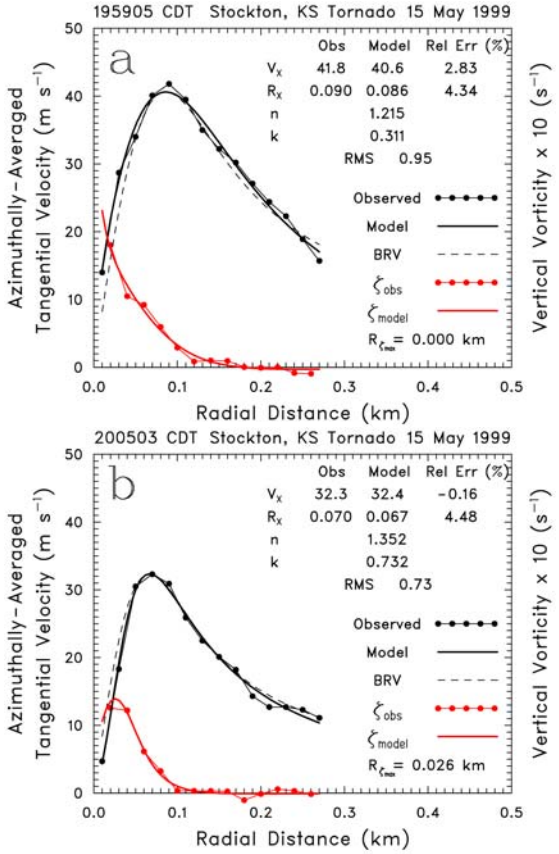

Fig. 4. Radial profiles of GBVTD-analyzed azimuthally-averaged (black dot-line curve) and analytical (black, solid curve) tangential velocity, GBVTD-analyzed (red, dot-line curve) and analytical vertical vorticity (red, solid curve) at (a) 19:59:05 and (b) 20:05:03 CDT. The height and range of the radar beam at the estimated vortex center, respectively, are (a) 0.09 and 4.80 km and (b) 0.12 and 6.45 km. Dashed curve refers to the Burgers (1948)-Rott (1958) tangential velocity profile for comparison purpose. Relative errors (%) and RMS errors (m s^{-1}) between the observed and model parameters are indicated.

5. SUMMARY

An analytical model of one- and two-celled vortices is presented in which four parameters dictate the shape of the tangential velocity profile, and hence, the vertical vorticity profile. Comparison of the fitted profiles and those analyzed or derived from Doppler radar observations shows good agreements. A couple of conclusions can be drawn from this study:

1) The model parameter k determines the concavity of the tangential velocity profile near the vortex center. When $k \le 0.5$ ($k > 0.5$), the tangential velocity profile near the vortex center has negative (positive) curvature [curve turns to right (left) with increasing r] and vertical vorticity is maximum at the center (between the center and the core radius), suggestive of a one-celled (two-celled) vortex.
2) Another model parameter n dictates the decay rate of the profile (rate at tangential velocity decays with increasing radial distance). When n (which always exceeds k) is small, the tangential velocity profile outside the core radius is nearly flat (i.e., small decay rate). Increasing the n values increases the decay rate.

6. FUTURE STUDIES

This preliminary study is the first part of the ongoing research. Future studies will include a new analytical expression for a radial velocity component. The component, currently being developed, will be used to obtain a vertical velocity distribution, via a two-dimensional continuity equation. The radial and vertical velocity components will describe one- and two-celled circulations. More mobile Doppler radar measurements of tornadoes will be used to test against the fitted parameters of the analytical model.

7. ACKNOWLEDGMENTS

The lead author would like to thank Bob Davies-Jones for reading and making input and suggestions in this paper.

10. REFERENCES

Alexander, C. R. and J. Wurman, 2005: The 30 May 1998 Spencer, South Dakota, Storm. Part I: The structural evolution and environment of the tornadoes. *Mon. Wea. Rev.,* **133,** 72-96.

Bluestein, H. B., C. C. Weiss, and A. L. Pazmany, 2004: Doppler radar

observations of dust devils in Texas. *Mon. Wea. Rev.,* **132,** 209-224.

Burgers, J. M., 1948: A mathematical model illustrating the theory of turbulence. *Adv. Appl. Mech.*, **1,** 197-199.

Davies-Jones, R. P., 1986: Tornado dynamics, in *Thunderstorm Morphology and Dynamics,* 2nd ed., edited by E. Kessler, University of Oklahoma Press, Norman, 197-236.

Gerald, C. F., and P. O. Wheatley, 1984: *Applied Numerical Analysis.* 3rd ed. Addision-Wesley Publishing Company, 579 pp.

Lee, W.-C., and J. Wurman, 2005: Diagnosed three-dimensional axisymmetric structure of the Mulhall tornado on 3 May 1999. *J. Atmos. Sci.,* **62,** 2373-2393.

_____, J.-D. Jou, P.-L. Chang, and S.-M. Deng, 1999: Tropical cyclone kinematic structure retrieved from single-Doppler radar observations. Part I: Doppler velocity patterns and the GBVTD technique. *Mon. Wea. Rev.,* **127,** 2419-2439.

Rankine, W. J. M., 1901: *A Manual of Applied Mechanics.* 16th ed. Charles Griff and Co., 680 pp.

Rott, N., 1958: On the viscous core of a line vortex. *Z. Angew. Math. Physik,* **96,** 543-553.

Rotunno, R., 1977: Numerical simulation of a laboratory vortex. *J. Atmos. Sci.,* **34,** 1942-1956.

_____, 1984: An investigation of a three-dimensional asymmetric vortex. *J. Atmos. Sci.,* **41,** 283-298.

Sullivan, R. D., 1959: A two-cell vortex solution of the Navier-Stokes equations. *J. Aerospace. Sci.*, **26,** 767-768.

Tanamachi, R. L., H. B. Bluestein, W.-C. Lee, M. Bell, and A. Pazmany, 2006: Ground-based velocity track display (GBVTD) analysis of W-band Doppler radar data in a tornado near Stockton, Kansas on 15 May 1999. *Mon. Wea. Rev*. (In press).

Wurman, J., 2002: The multiple-vortex structure of a tornado. *Wea. Forecasting,* **17,** 473-505.

_____, and S. Gill, 2000: Finescale radar observations of the Dimmitt, Texas (2 June 1995), tornado. *Mon. Wea. Rev.,* **128,** 2135-2164.

_____, and C. R. Alexander, 2005: The 30 May 1998 Spencer, South Dakota, Storm. Part II: Comparison of observed damage and radar-derived winds in the tornadoes. *Mon. Wea. Rev.,* **133,** 97-119.